



Published in final edited form as:

J Cogn Neurosci. 2010 June ; 22(6): 1299–1318. doi:10.1162/jocn.2009.21261.

Single-trial fMRI Shows Contralesional Activity Linked to Overt Naming Errors in Chronic Aphasic Patients

Whitney Anne Postman-Caucheteux¹, Rasmus M. Birn¹, Randall H. Pursley¹, John A. Butman¹, Jeffrey M. Solomon², Dante Picchioni³, Joe McArdle¹, and Allen R. Braun¹

¹National Institutes of Health, Bethesda, MD

²Medical Numerics, Inc., Germantown, MD

³Walter Reed Army Institute of Research, Silver Spring, MD

Abstract

We used fMRI to investigate the roles played by perilesional and contralesional cortical regions during language production in stroke patients with chronic aphasia. We applied comprehensive psycholinguistic analyses based on well-established models of lexical access to overt picture-naming responses, which were evaluated using a single trial design that permitted distinction between correct and incorrect responses on a trial-by-trial basis. Although both correct and incorrect naming responses were associated with left-sided perilesional activation, incorrect responses were selectively associated with robust right-sided contralesional activity. Most notably, incorrect responses elicited overactivation in the right inferior frontal gyrus that was not observed in the contrasts for patients' correct responses or for responses of age-matched control subjects. Errors were produced at slightly later onsets than accurate responses and comprised predominantly semantic paraphasias and omissions. Both types of errors were induced by pictures with greater numbers of alternative names, and omissions were also induced by pictures with late acquired names. These two factors, number of alternative names per picture and age of acquisition, were positively correlated with activation in left and right inferior frontal gyri in patients as well as control subjects. These results support the hypothesis that some right frontal activation may normally be associated with increasing naming difficulty, but in patients with aphasia, right frontal overactivation may reflect ineffective effort when left hemisphere perilesional resources are insufficient. They also suggest that contralesional areas continue to play a role—dysfunctional rather than compensatory—in chronic aphasic patients who have experienced a significant degree of recovery.

INTRODUCTION

Neuroimaging research of language recovery in people with aphasia due to left hemisphere damage has generated some intriguing results, yet crucial questions remain about the contributions of perilesional and contralesional brain areas to linguistic performance. Many studies have converged upon a model in which the best outcomes are associated with an

approximation to the dominant pattern observed in neurologically intact subjects, with mainly left hemisphere activation during language production tasks (Heiss, Thiel, Kessler, & Herholz, 2003; Perani et al., 2003; Cao, Vikingstad, George, Johnson, & Welch, 1999; Warburton, Price, Swinburn, & Wise, 1999; Belin et al., 1996).

In some people with aphasia, right hemisphere regions homologous to left-sided language areas have been found to be significantly activated for sentence reading (Thulborn, Carpenter, & Just, 1999) and auditory narrative comprehension (Crinion, Warburton, Lambon-Ralph, Howard, & Wise, 2006). Although the capacity of right hemispheric areas to compensate for left-sided damage may be greater for comprehension than production, right frontal activation has been proposed to subserve overt repetition (Ohyama et al., 1996) and silent word generation (Blasi et al., 2002) in aphasic patients. Increasing bilateral activation has also been linked to improvement in overt word generation (Cardebat et al., 2003). Other studies have suggested that contralesional involvement in language performance may result from release of trans-callosal inhibition from damaged left-sided areas, without being effective (Blank, Bird, Turkheimer, & Wise, 2003; Rosen et al., 2000). The roles proposed for contralesional and ipsilesional areas in aphasia recovery are not necessarily in opposition but rather may depend upon factors such as severity of aphasia, degree of rehabilitation, and time course of recovery (Crosson et al., 2007).

A major obstacle to investigating the neural basis for language production in aphasia has been lack of monitoring of patients' performance on a single-trial basis during image acquisition, precluding error analyses. With PET, overt responses cannot be evaluated on a single-trial basis; therefore, analyses are restricted to measures of overall accuracy (Cardebat et al., 2003). In fMRI studies with BOLD imaging of language production, participants have often performed tasks covertly to avoid motion and susceptibility artifacts due to articulatory movements, and performance level must be assessed off-line (Perani et al., 2003; Blasi et al., 2002).

Three recent fMRI studies notable for acquiring overt picture-naming responses in people with aphasia offer apparently contradictory results. Meinzer et al. (2006), implementing a sparse sampling technique in a single patient, reported more right frontal activation for her correct than her incorrect responses after therapy. In a treatment study with two patients with phonological anomia, Vitali et al. (2007) described distinct patterns of activation associated with training. In the event-related fMRI session subsequent to therapy, a young adult patient with aphasia secondary to closed head injury showed greater perilesional activation, whereas an older adult patient with aphasia secondary to stroke showed greater activation predominantly in right Broca's homologue. In contrast, Martin et al. (2005), using a block design, showed more left-sided activation in patients with high naming accuracy and more right-sided activation in a poorly performing patient. Also using a block design with overt speech, Léger et al. (2002) observed an increase in left perilesional areas in a patient with aphasia after phonemic articulation therapy. Recently, BOLD fMRI studies of single word production with neurologically intact subjects have overcome complications due to articulation with a novel event-related paradigm using continuous EPI (Birn, Cox, & Bandettini, 2004; Birn, Bandettini, Cox, & Shaker, 1999), yet thus far they have not been

implemented with patients with aphasia. In our study, we adapted this paradigm for use with such participants.

Another potential confound in studies of poststroke aphasia arises when a cohort of patients is analyzed as a group, a procedure typically used in studies of subjects without structural lesions. This procedure is problematic because information about individual patterns of activation can be lost through averaging of patient brain images (Rosen et al., 2000). Therefore, analysis of individual cases is likely to be critical for fully appreciating the details of activation patterns when lesions are present. This is the approach taken in the present study.

An emerging theory is that the time course of stroke recovery is such that reliance upon contralesional structures may be greater in earlier stages (Saur et al., 2006; Fernandez et al., 2004; Heiss, Kessler, Thiel, Ghaemi, & Karbe, 1999), reflected in activation of these structures in the acute poststroke phase. Functional recovery is associated with emerging activation of perilesional tissue, which is achieved through improvement of metabolic rate, regression of diaschisis, reduction of edema, and neuroplastic reorganization with time. Thus, in studies that include acute or subacute patients, time-dependent activity in perilesional and contralesional regions will be obscured in intersubject averaging. On the other hand, the notion that right hemisphere activation is exclusively associated with the period immediately following infarction cannot adequately address the findings of significant right-sided activation in some chronic aphasia patients many years after onset, particularly those with large left peri-sylvian lesions (Blasi et al., 2002; Cao et al., 1999). Because patients can survive for decades after stroke onset, it is worth asking what the role of the right hemisphere is in long-term chronic aphasia, especially when a significant degree of recovery has been achieved. In the present study, we addressed this question by testing patients who were at least 3 years after onset and who had made substantial linguistic gains since the acute poststroke phase.

Finally, the choice of different tasks across studies has complicated comparison of results and generalization of conclusions. Some tasks may have only an indirect relationship to natural language performance, and well-tested psycholinguistic models of the processes involved in executing them are seldom considered. In this fMRI study, we selected overt picture naming for the functional task because it has been extensively used in clinical evaluations and behavioral experiments with people with aphasia as a measure of word-finding difficulty, the most pervasive symptom across all types of aphasia. Excellent models have been developed to identify the psycholinguistic processes underlying both intact and impaired picture-naming performance, such as the theory of lexical access proposed by Levelt (2001) and the interactive two-step model of lexical access as described by Schwartz, Dell, Martin, Gahl, and Sobel (2006; for a review, see Gordon, 1997), to which we refer in our analysis of the participants' performance during scanning.

We used fMRI to examine the role of the contralesional (right) hemisphere in chronic aphasic patients who had achieved high levels of recovery but still manifested aphasic symptoms, particularly in production. We studied patients selected from a larger cohort, in whom the frequency of errors was sufficient to statistically compare correct and incorrect

“pseudopictures,” distortions of the original object pictures, were presented during each of the runs but will not be considered here.

Data Acquisition

Gradient-echo echo-planar images were acquired with BOLD imaging on a 3-T whole-body scanner (GE Signa; General Electric, Milwaukee, WI) with a standard quadrature head coil. The scan parameters were as follows: repetition time (TR) = 2000 msec per volume, echo time (TE) = 30 msec, flip angle = 90°, matrix = 64 × 64, field of view = 220 mm, 23 parallel axial slices covering the whole brain at 6-mm thickness, no gap. Four dummy scans were acquired at the start of each run to allow the magnetic resonance signal to reach an equilibrium state. Each of the eight runs acquired for each subject comprised 132 volumes (4 min 32 sec). T1-weighted MP-RAGE structural images (axial plane, TE = 30 msec, flip angle = 6°, field of view = 22 cm, slice thickness = 1.5 mm, 128 slices) were obtained before acquisition of functional data for registration of functional maps to anatomical images.

Participants lay supine in the scanner, wearing ear cuffs to which a fiber-optic dual-channel noise-canceling microphone (Optoacoustics, Ltd., Or-Yehuda, Israel) was attached and suspended above their lips. Subjects' heads were further secured with foam padding. During scanning, their overt responses were sampled through one microphone (signal plus noise) whereas the other microphone, perpendicular to the first, was used to sample only scanner noise. Data from both channels were deterministically processed with Opticlear software and saved to the laptop. In addition, the software saved the original data from the microphones and the stimulus onset times. All files were saved as WAV files at a sampling rate of 8 kHz with 16-bit resolution.

Afterwards, the original data from the microphones were reprocessed using custom adaptive noise cancellation software to enhance the clarity of the overt responses (R.P.). The software is based on the time-domain least mean squared adaptive filter algorithm. The algorithm uses a filter on the noise channel and subtracts this from the overt response channel. The resulting signal is the filtered overt response and is also used as feedback to change the coefficients of the filter used on the noise channel. As the filtered overt response becomes clearer, the filter coefficients change in smaller increments until they reach a steady state, at which point the filter is optimized and the mean squared error of the filtered overt response is as small as possible for the selected number of filter coefficients (i.e., noise is minimized). In this case, the number of filter coefficients was selected through trial and error to reduce the noise component of the filtered overt responses by approximately 20 dB.

Picture stimuli were projected onto a screen with Presentation software (Neurobehavioral Systems, Albany, CA) and were visible to subjects through a head-mounted mirror (visual angle = 7.6° vertically, 10.2° horizontally). They were presented with an 800-msec duration and a between-picture ISI ranging from 4 to 8 sec, jittered by 1-sec intervals. Each stimulus onset was accompanied by a pulse received by the Optoacoustics hardware, saved as a WAV file, and used off-line in our calculation of verbal response latencies. Black-and-white pictures of objects were presented against a white background in each of the eight runs. Between pictures, subjects fixated on a black crossbar centered on a white screen. After presentation of a series of nine pictures, the crossbar remained onscreen for 20 sec, allowing

the hemodynamic response of subjects to return to baseline. Even with these longer rest periods, a series of picture-naming trials were not analyzed as blocks. Rather, each picture-naming trial was analyzed as a single event, as permitted by ISIs of 4, 5, 6, 7, or 8 sec. A transistor-transistor logic (TTL) level pulse from the scanner triggered the start of each scenario, thus synchronizing the scenario to the scanner.

Data Processing

Data analysis was performed using the Analysis of Functional Neuroimages (AFNI; Cox, 1996). The eight functional files for each subject were time shifted to compensate for acquisition delays and volume registered to a base volume in the first run. The output of volume registration was evaluated for excessive head movement and saved into a file containing the adjustments in all six parameters to be included in the deconvolution analysis as regressors of no interest. Functional images were then blurred to a root mean square of 6-mm width and masked to remove background noise. The eight resulting masks were compiled into a full mask that was applied to the scaling algorithm by creating a voxelwise mean for each functional image, dividing voxel values by the resulting means and multiplying by 100, then multiplying by the full mask. Thus, voxel values were transformed into percent signal change. The eight volume-registered, blurred, masked, and scaled functional runs were then concatenated into a single data set for each subject.

A whole-brain analysis method was used. For each subject, deconvolution analysis was performed with the concatenated functional data set as input to permit computation of hemodynamic response function from the data without assumption of standard hemodynamic response function (HRF), estimated up to 12 sec poststimulus ($\min_{lag} = 0$, $\max_{lag} = 12$) at lags of half TR (1 sec). Given the length of the runs (4 min 32 sec), a second-order (quadratic) polynomial was included in the regression equation to control for baseline drift. The regressors in the deconvolution analysis included the six motion parameters and the stimulus timing files with precise onset timings for (1) all picture stimuli, analyzed separately from (2) only the pictures to which subjects responded correctly and (3) only the pictures to which subjects responded incorrectly. Impulse response functions for each stimulus time series were estimated and included in the output file.

General linear tests were used to analyze the following contrasts: (1) naming minus rest, the difference in activation between all responses to object pictures (whether accurate or inaccurate) and cross-fixation; (2) incorrect naming minus rest, the difference in activation between trials in which subjects provided inaccurate responses and cross-fixation; (3) correct naming minus rest, the difference in activation between trials in which subjects provided accurate responses and cross-fixation; and (4) correct naming versus incorrect naming, identifying activity greater for either accurate or inaccurate responses. For all contrasts, the area under the curve was calculated between 3 and 10 sec poststimulus onset to ignore time points most likely to include task-related motion artifact soon after stimulus onset as well as time points after expected HRF peak, when difference between amplitude and baseline should be minimal. Maps resulting from contrasts of correct and incorrect responses were generated with inclusive masking, whereby only activation surviving a

specified threshold ($p < .01$) for both correct responses minus rest and incorrect responses minus rest was included in the calculations.

For patients, all contrasts were calculated using an individual subject analysis, respecting anatomical and lesion variability in patients. Conversely, images for the healthy control participants were submitted to both subject-specific and group analyses. Data sets were registered to standard Talairach–Tournoux space (Talairach & Tournoux, 1988) using the manual transformation mode in AFNI, which involves marking anatomical locations for alignment of anterior and posterior commissures, then scaling to Talairach–Tournoux atlas brain size. Overall significance level was estimated with Monte Carlo simulation for generated functional images by estimating spatial correlation of voxels with Gaussian filtering, thresholding voxels at .001, masking and cluster identification at an alpha level of .05, for both subject-specific and group contrast images. A two-factor ANOVA was performed on the control subject data sets, using a mixed effects model (fixed condition, random subjects).

As a post hoc analysis motivated by the finding that certain properties of picture stimuli significantly affected response accuracy in patients, especially the number of possible names per picture and the AoA of target name, we used the amplitude modulated regression in AFNI (<http://afni.nimh.nih.gov/>) to discover if the BOLD response amplitude varied proportionally to these properties in patients and control subjects. On the assumption that the effects of these stimulus properties on the fMRI signal are linearly proportional to the changes in the values of these properties, two maps were created according to two separate regressors—the mean fMRI response and the deviations from the mean. The second map indicates brain areas where BOLD response is modulated by changes in the values of the stimulus properties. Using two regressors allows separation of voxels that are active but not detectably modulated by the stimulus properties of interest, from those that are sensitive to these properties. AM regression maps were created with a voxelwise threshold of $p < .05$, uncorrected.

Dynamic Susceptibility Scans

Relative cerebral perfusion was estimated with dynamic susceptibility contrast MRI to track a bolus of intravenous Gd-DTPA. Whole-head dynamic susceptibility contrast MRI was performed using two-dimensional gradient-echo echoplanar slices, repeated every 2 sec for at least 60 sec before, during, and after bolus administration of 0.1 mmol/kg Gd-DTPA at 3–5 ml/sec iv. Acquisition parameters were as follows: TR = 2000 msec, TE = 50 msec, and flip angle = 90°. Geometric parameters were as follows: field of view = 220 mm, matrix = 128 × 96, slice thickness = 5 mm, gap = 0 mm. Parametric maps of relative CBF, cerebral blood volume, and mean transit time were estimated from these data by pixelwise conversion of signal intensity into Gd concentration and subsequent deconvolution with an estimated arterial input function derived from voxels in the intracranial vessels using an automated algorithm in MEDx (v 3.44; Medical Numerics Inc., Germantown, MD). Whereas for the other analyses images were transformed to standard space, perfusion analyses were conducted in native space to avoid lesion distortion because their focus was on perilesional tissue.

RESULTS

Aphasic patients presented with slow and effortful speech but excellent comprehension (Table 1). According to the WAB (Kertesz, 1982), Patient 1, a 68-year-old Caucasian woman 9 years after onset of a large left MCA infarction, was classified as having conduction aphasia. Patient 2 was a 63-year-old Caucasian man classified as having anomic aphasia due to left anterior and MCA infarction 4 years before testing. Patient 3, a 48-year-old African American woman, was classified as having anomic aphasia due to stroke with occlusion of the superior temporal branch of the left MCA, incurred 3 years before testing. Results from selected subtests of single word production and comprehension from the WAB, the Psycholinguistic Assessments of Language Processing in Aphasia (Kay, Lesser, & Coltheart, 1992), and the Psycholinguistic Assessment of Language (Caplan, 1992) indicate that patients had some difficulty with name production but not comprehension. On the spontaneous speech subtest of the WAB, all three patients were matched on scores of information content (8 on a scale of 10), but on the measure of fluency, Patient 1 scored lower (6 on scale of 10) than Patients 2 and 3 (8 on scale of 10).

Structural (MP-RAGE) scans obtained during the same session as the fMRI scans were further examined with the analysis of brain lesion software (Solomon, Raymont, Braun, Butman, & Grafman, 2007). Lesions were manually outlined slice by slice, and the tracings were reviewed by a neuroradiologist (J. A. B.). Images were deskulled and registered to the T1 MNI brain (standard of the International Consortium for Brain Mapping) then transformed to lesion-only images. The lesions were then intersected with the automated anatomical labeling (AAL) atlas (Tzourio-Mazoyer et al., 2002) to provide reports of lesioned AAL atlas areas (Table 2). Because no damage was incurred in the right hemisphere for any of the patients, only left hemisphere information is presented in the table. All three participants had significant involvement of left frontal, parietal, and insular regions. Patient 1 showed more involvement of middle and inferior frontal orbital gyri, Patient 2's lesion extended more anteriorly and subcortically, and Patient 3 had the most involvement of the superior temporal gyrus and supramarginal gyrus but the least involvement of the triangular gyrus and insula (presented in native space for accurate representation of the lesions on the structural images in Figure 1).

Psycholinguistic Analysis of Picture-naming Performance during fMRI

Overt responses for the picture-naming task during scanning permitted scoring and detailed analyses of participants' performance. Voice recordings were transcribed and scored independently by two raters. Although neurologically intact subjects produced almost no errors, the patients achieved 53% to 76% correct responses. Aphasic patients' errors were mostly semantic paraphasias (e.g., blimp → airplane; moose → deer; policeman → robber; jack → car) or omissions (Table 3). Omissions usually consisted of utterance of formulaic expressions and pause fillers (e.g., dunno, no idea, um uh oh, oh man!). Occasional phonemic errors include spaghetti → pasketti, binoculars → nonoculars. Only two errors were nonnominal: pool → swim; drill → electric. No perseverations were observed.

Of the 144 picture stimuli, those inducing semantic and omission errors were characterized by two variables, late AoA and high number of alternative names. AoA correlated

significantly with omissions (Pearson correlation = .24, $p = .0004$, two tailed), the number of alternative names correlated significantly with semantic paraphasias (Pearson correlation = .21, $p = .01$, two tailed) and with omissions (Pearson correlation = .29, $p = .0005$, two tailed), and, these two measures correlated with each other (Pearson correlation = .26, $p = .0002$, two tailed). Examples of pictures with late AoA that induced omissions were tank and hinge. Examples of pictures with high number of alternative names that induced semantic paraphasias were knot → rope, pretzel and city → village, building. The pictures with low number of alternative names and/or early AoA that were correctly named by all three patients were basket, butter, mushroom, nose, pirate, rocking chair, stroller, toothbrush, and tree. No other stimulus variables (semantic category, name frequency, length in syllables of dominant name, and visual complexity of pictures) predicted patients' naming errors, although it is noteworthy that frequency inversely correlated with AoA (Pearson correlation = $-.27$, $p = .0001$, two tailed).

Length in syllables of patients' accurate and inaccurate responses did not differ significantly, averaging 2.15 ± 1.2 syllables for accurate responses and 2.3 ± 1.3 syllables for inaccurate responses, including particles such as "um" and "uh." Average naming response latencies for the aphasic patients were 2.6 ± 0.2 sec on accurate trials and 3.0 ± 0.2 sec on inaccurate trials, with the difference approaching significance ($p < .06$, two-tailed t test).

Functional Results for Healthy Age-matched Control Subjects

Subject-specific analyses of control subjects' data showed consistent patterns of activation (Figure 2, above). For all control subjects, overt picture naming activated visual areas, posterior peri-sylvian areas, thalamus, and BG, with robust left lateralization in inferior frontal gyrus (IFG) and insula. In the cohort analysis (Figure 2, below and Table 4), local maxima in relevant areas of the left hemisphere were found in inferior, middle, superior, and medial frontal gyri, precentral gyrus. There were fewer maxima in the right hemisphere, and these were located in the superior and middle frontal gyri and precentral gyrus.

Functional Results for Patients with Aphasia—General Pattern for All Trials

Perilesional and contralesional activation for all trials was seen in all three patients (Figure 3). Impulse response functions from activated perilesional voxels estimated in AFNI showed a standard HRF shape. As illustrated in the impulse response function (IRF) graphs in Figure 4, the range of values for percent signal change (1–2%) and times to peak (4–5 sec) were characteristic of nonartifactual responses. Images in Figure 4 are displayed in native space (without stereotaxic normalization) to precisely single out perilesional voxels without compromising integrity of lesion extent and shape (Table 5).

Dynamic Susceptibility Results for Patients with Aphasia

Dynamic contrast studies demonstrated perilesional perfusion in all three patients (Figure 5, images displayed in native space to preserve integrity of lesion extent and shape). This suggests that in these regions, a hemodynamic response would be supported by adequate flow and that the observed activation is real rather than an artifact of susceptibility.

Functional Results for Patients with Aphasia—Comparison of Accurate and Inaccurate Trials

As a next step, correct and incorrect trials were directly contrasted to determine if neural activation was modulated by accuracy. BOLD contrasts comparing correct and incorrect responses showed that perilesional activations were not systematically modulated by response accuracy (Figure 6). That is, both accurate and inaccurate responses activated left-sided regions, and the magnitude of activation did not differ between response types. In contrast, responses in the right hemisphere were significantly modulated by response accuracy. Patients' incorrect responses were associated with activation of contralesional prefrontal areas, whereas correct responses were not. Contrasts of incorrect minus fixation versus correct minus fixation responses reveal significantly greater BOLD responses in right contralesional areas, chiefly in the right inferior and middle frontal gyri (Tables 6 and 7).

Modulation of BOLD Amplitude by Psycholinguistic Measures

As the AoA and the number of alternative names per target were significantly associated with patients' errors, we used amplitude modulated regression methods in AFNI (see Methods) to identify regions in which the BOLD response varied proportionally to these measures. In all three patients, variations in these two measures modulated BOLD signal amplitude, indicating that these areas are especially sensitive to these naming characteristics. Later AoA and greater number of alternative names per target were each associated with greater responses in perilesional and frontal contralesional areas, including inferior and middle frontal gyri, and a similar pattern obtained for the four control subjects (Figure 7). These amplitude changes were relatively small, peaking around 0.05% signal change. For this reason, maps are shown at voxelwise threshold of $p < .05$, uncorrected (Tables 8–11).

DISCUSSION

Using an overt picture-naming paradigm and fMRI, we investigated patterns of brain activation in three aphasic patients, selected from a larger cohort, in whom the frequency of errors was sufficient to statistically compare correct and incorrect trials. Four age-matched control subjects were also studied. The patients were well-recovered but still noticeably aphasic, allowing us to compare the roles of perilesional and contralesional activation for language production long after the most dramatic changes in post-stroke brain reorganization are supposed to have occurred (Cramer, 2004) and recovery is assumed to plateau (Kertesz, 1984). Our results inform and augment the growing body of research on the neural substrate for language production in aphasic stroke patients, allowing for the direct comparison of correct and incorrect responses acquired on a trial-by-trial basis. We chose picture naming because this psycholinguistically valid task is part of every standard aphasia battery and has a long history as an investigative tool in the study of speech errors in healthy subjects and patient populations (Schwartz et al., 2006; Gordon, 1997), upon which we based our analysis of participants' performance.

For the four age-matched healthy control subjects, all of whom performed at ceiling, individual and cohort analyses revealed a definite pattern of left-lateralized peri-sylvian activation (Figure 2). Robust left-sided activation was evidenced in all three aphasic

patients, including the region of the peri-infarct rim, despite the presence of extremely large left hemisphere lesions in the first two cases (Figure 3). This perilesional activation was confirmed as real and not artifact by inspection of the IRF curves in activated voxels around the rim of the lesion that exhibited morphologies, response latencies, and percent signal changes characteristic of real hemodynamic response (Figure 4) and detection of flow in the same areas in dynamic susceptibility studies (Figure 5). Careful inspection and cautious interpretation of the hemodynamic responses in brain-damaged patients are essential because in some cases these can be highly deviant (Bonakdarpour, Parrish, & Thompson, 2007). Our results agree with those of a number of neuroimaging studies showing perilesional activation in well-recovered chronic patients on production tasks (Perani et al., 2003; Cao et al., 1999; Warburton et al., 1999; Belin et al., 1996).

In addition to robust perilesional activation, right hemisphere activation in regions roughly opposite to the left hemisphere damage was observed in all three patients (Figure 3). The right frontal activation was a striking point of distinction between patients and controls. In all three patients, accurate performance was associated with a pattern of activation that approximated the left-lateralized pattern observed in the healthy age-matched control subjects, a result that is in agreement with recent findings about good stroke recovery (Cramer, 2004). On the other hand, virtually no activation in areas contralateral to left frontal activation was observed in controls and was seen almost exclusively during production of inaccurate responses in the participants with aphasia (Figure 6). This finding generally concurs with studies that have reported right frontal activation during language production in aphasic patients (Blank et al., 2003; Blasi et al., 2002; Rosen et al., 2000; Ohyama et al., 1996), although our experiment is the first to correlate it with inaccurate performance. We consider in turn each of the studies demonstrating contralesional activation and how they relate to our results.

In a PET study of narrative production by Blank et al. (2003), chronic patients with damage to left pars opercularis (POp) showed activation in right POp that was not seen in patients without damage to the same area or in control subjects. As the healthy subjects showed a decrease in activation in right POp, the authors concluded that transcallosal inhibition from the stroke to the nonstroke hemisphere was lost in left POp patients. A similar conclusion was reached by Rosen et al. (2000) in their fMRI and PET investigations of word-stem completion and pseudoword reading in patients with left frontal damage. Blank et al. noted that the left POp patients' language performance was slower and less syntactically complex than that of the other two groups and that with no direct evidence that the observed right POp activation was supporting their propositional speech, it could reasonably be attributed to effort. This conclusion is in accord with our results as well as those of Naeser et al. (2004), in which overt propositional speech was elicited from patients with nonfluent aphasia as they underwent contrast-based fMRI scans and activation in the right SMA and in the right peri-sylvian regions was related to their production difficulties and deficits.

Blasi et al. (2002) interpreted attenuation of contralesional activity with training on silent word-stem completion as evidence for a compensatory role of the right hemisphere. However, it is notable that three of their patient participants, who had smaller lesions and showed perilesional activation, performed better than those whose lesions were larger and

who showed more right-sided activation (replicating results from two patients in Rosen et al., 2000). Blasi et al. proposed that the patients showing the most right frontal activation may be implementing a visual/orthographic strategy to accomplish the task, whereas the observed left frontal activation may support a linguistic/phonological strategy. According to this proposal, the right hemisphere may support separate capacities that operate as alternative, compensatory strategies when left hemisphere structures supporting language generation are damaged.

In the PET study of word repetition by Ohyama et al. (1996), more right frontal and temporal activation was observed in participants with nonfluent aphasia than controls. This finding might be related to the fact that their study included patients at 4 months or less after onset, for whom contralesional activation may have eventually receded as recovery progressed (as suggested in, e.g., Saur et al., 2006). Moreover, Ohyama et al. reported that good performance by patients on spontaneous speech tasks as measured off-line correlated with *left* hemisphere rCBF. This overlooked result is consistent with the notion that left hemisphere activation is an essential component of good poststroke recovery of language production.

Three recent studies that, like ours, investigate overt picture-naming with fMRI in patients with aphasia deserve mention. Although the blocked design experiment by Martin et al. (2005) did not allow for direct comparison of accurate to inaccurate responses, their findings of greater and more extensive right hemisphere activation in the severely impaired patient who produced only inaccurate responses are consistent with our results. In the recovery studies by Vitali et al. (2007) and Meinzer et al. (2006), patients were scanned before and after treatment for anomia. The single patient in the former investigation and the patient with aphasia due to stroke in the latter both showed right inferior frontal activation on trained items increasing with accuracy, alongside left perilesional or left frontal activation. Although at first blush their results may seem contradictory to ours, they may not be fully comparable and may even be complementary.

Meinzer et al. (2006) used a sparse temporal sampling technique, which avoids the motion and susceptibility artifacts associated with overt speech but does have the drawbacks of requiring the patient to respond during the 3-sec interval between stimulus presentation and image acquisition and considerably reducing the number of trials due to the lengthy ISI (minimum 9 sec). Our continuous scanning technique, in which the impact of artifact is mitigated by the distinctive time courses of motion-induced artifact and hemodynamic response (Birn et al., 1999, 2004), allows for an ample number of trials with a range of shorter ISIs (4–8 sec). The participants in our study had anomic or conduction aphasia, they achieved at least 50% correct responses on the fMRI naming task, and never produced neologisms, an error-type characteristic of more severe aphasic impairment (Schwartz et al., 2006). In contrast, the patient in the study of Meinzer et al. was classified with Wernicke's aphasia, achieved less than 30% correct names even after treatment, and produced a substantial number of neologisms. Similarly, many of the errors produced by the stroke patient with phonological anomia in Vitali et al. (2007) were phonemic approximations, an error-type characteristic of deeper naming deficit. Therefore, it may be the case that right

frontal activation is more vital for poorly recovered patients but less so for good performance in well-recovered patients.

In a subsequent study by Meinzer et al. (2008) with a group of chronic patients, areas of excessively slow delta wave activity concentrated in left perilesional regions were identified with magneto-encephalographic exams. Comparison of pretreatment and posttreatment fMRI scans revealed a correlation between improvements in naming of pictures trained during intensive language therapy and increasing activation in these slow wave perilesional regions. Their conclusion that restoration or reintegration of perilesional tissue plays a central role in language improvement even in chronic aphasia is in agreement with our results.

The major finding of the present study is the link between incorrect naming responses, including both para-phasias and omissions, and right frontal activation in three chronic, well-recovered patients with aphasia due to stroke in left fronto-parietal cortices. The difference in activation patterns cannot be due to longer utterances for incorrect responses because correct and incorrect responses were almost identical in length. Latencies for inaccurate responses were on average somewhat longer than those for accurate responses, a result that supports the notion that errors were related to increased naming difficulty. It is unlikely, however, that these latency differences account for the larger contralesional responses we observed. The mean latency gap between accurate and inaccurate responses of 0.4 sec is too small to produce a major shift in the hemodynamic response that could account for the observed difference in response amplitude in right frontal areas. According to our simulations in AFNI (R.B.), this small shift in the BOLD response would account for a difference in estimated response amplitude by a fraction up to 0.08%. Given that the effect that we observed is much greater, this must represent a true difference in response amplitude.

That the observed right frontal activation was driven by patients' errors casts doubt on the hypothesis that it is generally an effective compensatory mechanism for recovery. Critically, we are not contending that frontal contralesional activation is the source of patients' errors. Instead, our finding provides novel evidence supporting the hypothesis that contralesional activation may represent increased but less effective search and selection processes recruited when left perilesional areas are insufficient. Although right hemisphere activation in aphasic patients has already been proposed to represent "maladaptive effort" (Hillis, 2005), our qualitative analysis of patients' errors recorded on-line during the acquisition of fMRI data enabled us to better characterize the nature of this effort.

The effects of AoA and number of alternative names per target on patients' naming errors are expected based on previous findings on aphasia. Kittredge, Dell, Verkuilen, and Schwartz (2008) have argued for a link between omission errors and picture names with late AoA and attributed it to greater processing resources needed for retrieval of later learned word forms. Patients' greater difficulty on items requiring selection from a large set of possible responses is consistent with the proposed role of the left IFG in semantic selection (Kan & Thompson-Schill, 2004). We found that these measures affected fMRI activation

amplitude perilesionally and in right frontal regions in all three patients, indicating that these areas are especially sensitive to these naming characteristics (Figure 7).

In the psycholinguistic literature on picture naming, omissions are routinely counted and tracked as errors. Because they have been found to be related to semantic para-phasias in the frequency with which they occur in patients, combining both types of errors in our analyses of incorrect naming was reasonable. In a study employing a blocked cyclic naming paradigm, Schnur, Schwartz, Brecher, and Hodgson (2006) found that for a group of patients with Broca-type aphasia, both omissions and paraphasias were sensitive to semantic interference, in contrast to all other error types (e.g., neologisms, phonemic paraphasias, and circumlocutions). Schnur et al. concluded that both omissions and semantic paraphasias can arise as a consequence of unresolved interference due to increased competition. Our finding that both error types were induced by pictures with many possible target names agrees with the results of Schnur et al. and supports their explanation of patients' performance as a disruption of lexical selection.

Left and right frontal regions were affected by the measures of AoA and the number of names per target in the four healthy participants as well (Figure 7). This result is corroborated by those of an fMRI study with normal subjects of lexical decision using early and late learned words by Fiebach, Friederici, Müller, von Cramon, and Hernandez (2003), linking increased activation in portions of the left IFG with comprehension of late acquired words. Furthermore, in an fMRI study of past tense generation with healthy participants, Desai, Conant, Waldron, and Binder (2006) found more activation in left and right IFG for irregular than regular verbs, which they attribute to the greater task demands imposed by the more complex stimuli. Our results contribute to these findings of a consistent coupling of frontal activation with linguistic complexity. Further-more, they suggest that it is the same phenomenon observed in both healthy and impaired participants but that is inadequate to offset left hemisphere damage in patients with aphasia due to left cerebrovascular accident (CVA).

The connection between increased neural activation and greater task complexity has precedent in imaging studies of stroke. In an fMRI study of picture-word matching in patients with chronic aphasia, Fridriksson and Morrow (2005) found more extensive and elevated activation in the right homologue of Broca's area and right superior temporal gyrus (STG) for the more demanding condition with more stimuli and shorter response times, on which the patients performed worse. Our results are also consistent with human motor stroke studies, suggesting that contralesional activity observed during movement of the paretic limb in well-recovered stroke patients (Cramer et al., 1997) may reflect processes that operate in the normal brain, where unilateral hand movements elicit activity in both hemispheres as task complexity increases (Rao et al., 1993).

Alternatively, the right hemisphere activation observed for incorrect but not correct responses could be partially attributed to patients' generation of formulaic expressions (e.g., dunno, oh man!) in their omissions. Research comparing propositional and nonpropositional speech in patients and neurologically intact subjects indicates a right hemisphere substrate for the processing and production of formulaic expressions (Van Lancker Sidtis & Postman,

2006). Yet another possible explanation is that right frontal activation may obstruct good language production. This possibility was supported by research with repetitive transcranial magnetic stimulation (rTMS) focused on the right IFG. Naeser et al. (2005) demonstrated improved naming and propositional speech in some chronic nonfluent aphasic patients who underwent 10 sessions of slow rTMS over right pars triangularis. In a study with acute aphasic patients, Winhuisen et al. (2005) showed a positive effect for right IFG stimulation only in the most poorly performing patients, again connecting contralesional overactivation with more impaired linguistic capacity.

However interpreted, our results suggest that right frontal regions continue to be active in language production in chronic aphasia. The influential longitudinal work on aphasia recovery (Saur et al., 2006; Fernandez et al., 2004; Heiss et al., 1999), by asserting that good outcomes depend upon return of functionality of perilesional areas, may give the misleading impression that right hemisphere function is no longer a factor in well-recovered patients. Our results distinguishing activation for accurate and inaccurate performance suggest that right frontal areas still play a role—likely dysfunctional rather than compensatory—long after left perilesional areas have regained predominance in good language production.

This study demonstrates the feasibility of measuring activation separately for accurate and inaccurate performance with fMRI and the advantages of investigating overt production in people with chronic aphasia. The potential clinical utility of our methods is clear for monitoring aphasia recovery longitudinally and evaluating therapeutic interventions. We are encouraged by the prospect that the methods described here might yield new discoveries about the dynamic nature of the neural substrate for language at all stages of poststroke recovery in aphasia.

Acknowledgments

This work was supported by the Intramural Program of the National Institute on Deafness and Other Communication Disorders. We gratefully acknowledge the invaluable comments, critiques, and suggestions from three anonymous reviewers. The first author acknowledges John Pluta and the Center for Functional Neuroimaging at the University of Pennsylvania (NS045839) for support during the revision phase of this manuscript, and is indebted to Patricia Sokolove, Alex Martin and Bob Loeffler for their guidance and encouragement.

REFERENCES

- Belin P, Van Eeckhout P, Zilbovicious M, Rémy P, François C, Guillaume S, et al. Recovery from nonfluent aphasia after melodic intonation therapy: A PET study. *Neurology*. 1996; 47:1504–1511. [PubMed: 8960735]
- Birn RM, Bandettini PA, Cox RW, Shaker R. Event-related fMRI of tasks involving brief motion. *Human Brain Mapping*. 1999; 7:106–114. [PubMed: 9950068]
- Birn RM, Cox RW, Bandettini PA. Experimental designs and processing strategies for fMRI studies involving overt verbal responses. *Neuroimage*. 2004; 23:1046–1058. [PubMed: 15528105]
- Blank SC, Bird H, Turkheimer F, Wise RJ. Speech production after stroke: The role of the right pars opercularis. *Annals of Neurology*. 2003; 54:310–320. [PubMed: 12953263]
- Blasi V, Young AC, Tansy AP, Petersen SE, Snyder AZ, Corbetta M. Word retrieval learning modulates right frontal cortex in patients with left frontal damage. *Neuron*. 2002; 36:159–170. [PubMed: 12367514]

- Bonakdarpour B, Parrish TB, Thompson CK. Hemodynamic response function in patients with stroke-induced aphasia: Implications for fMRI data analysis. *Neuroimage*. 2007; 36:322–331. [PubMed: 17467297]
- Cao Y, Vikingstad EM, George KP, Johnson AF, Welch KM. Cortical language activation in stroke patients recovering from aphasia with functional MRI. *Stroke*. 1999; 30:2331–2340. [PubMed: 10548667]
- Caplan, D. *Language: Structure, processing and disorders*. Cambridge, MA: MIT Press; 1992.
- Cardebat D, Démonet JF, De Boissezon X, Marie N, Marie RM, Lambert J, et al. Behavioral and neurofunctional changes over time in healthy and aphasic subjects: A PET language activation study. *Stroke*. 2003; 34:2900–2906. [PubMed: 14615626]
- Cox RW. AFNI: Software for analysis and visualization of functional magnetic resonance neuroimages. *Computers and Biomedical Research*. 1996; 29:162–173. [PubMed: 8812068]
- Cramer SC. Functional imaging in stroke recovery. *Stroke*. 2004; 35:2695–2698. [PubMed: 15388899]
- Cramer SC, Nelles G, Benson RR, Kaplan JD, Parker RA, Kwong KK, et al. A functional MRI study of subjects recovered from hemiparetic stroke. *Stroke*. 1997; 28:2518–2527. [PubMed: 9412643]
- Crinion JT, Warburton EA, Lambon-Ralph MA, Howard D, Wise RJ. Listening to narrative speech after aphasic stroke: The role of the left anterior temporal lobe. *Cerebral Cortex*. 2006; 16:1116–1125. [PubMed: 16251507]
- Crosson B, McGregor K, Gopinath KS, Conway TW, Benjamin M, Chang YL, et al. Functional MRI of language in aphasia: A review of the literature and the methodological challenges. *Neuropsychology Review*. 2007; 17:157–177. [PubMed: 17525865]
- Desai R, Conant LL, Waldron E, Binder JR. fMRI of past tense processing: The effects of phonological complexity and task difficulty. *Journal of Cognitive Neuroscience*. 2006; 18:278–297. [PubMed: 16494687]
- Fernandez B, Cardebat D, Démonet JF, Joseph PA, Mazaux JM, Barat M, et al. Functional MRI follow-up study of language processes in healthy subjects and during recovery in a case of aphasia. *Stroke*. 2004; 35:2171–2176. [PubMed: 15297629]
- Fiebach CJ, Friederici AD, Müller K, von Cramon DY, Hernandez AE. Distinct brain representations for early and late learned words. *Neuroimage*. 2003; 19:627–637. [PubMed: 12880793]
- Fridriksson J, Morrow KL, Moser D, Baylis GC. Age-related variability in cortical activity during language processing. *Journal of Speech, Language, and Hearing Research*. 2006; 49:690–697.
- Fridriksson J, Morrow L. Cortical activation and language task difficulty in aphasia. *Aphasiology*. 2005; 19:239–250. [PubMed: 16823468]
- Gordon, B. Models of naming. In: Goodglass, H.; Wingfield, A., editors. *Anomia: Neuroanatomical and cognitive correlates, foundations of neuropsychology*. San Diego, CA: Academic Press; 1997. p. 31-64.
- Heiss WD, Kessler J, Thiel A, Ghaemi M, Karbe H. Differential capacity of left and right hemispheric areas for compensation of poststroke aphasia. *Annals of Neurology*. 1999; 45:430–438. [PubMed: 10211466]
- Heiss WD, Thiel A, Kessler J, Herholz K. Disturbance and recovery of language function: Correlates in PET activation studies. *Neuroimage*. 2003; 20:S42–S49. [PubMed: 14597295]
- Hillis AE. Can shift to the right be a good thing? *Annals of Neurology*. 2005; 58:346–348. [PubMed: 16130102]
- Kan IP, Thompson-Schill SL. Effect of name agreement on prefrontal activity during overt and covert picture naming. *Cognitive Affective Behavioral Neuroscience*. 2004; 4:43–57.
- Kay, J.; Lesser, R.; Coltheart, M. *Psycholinguistic assessments of language processing in aphasia*. New York: Psychology Press; 1992.
- Kertesz, A. *The Western Aphasia Battery*. San Antonio: Harcourt Assessment Inc; 1982.
- Kertesz A. Recovery from aphasia. *Advances in Neurology*. 1984; 42:23–39. [PubMed: 6209949]
- Kittredge AK, Dell GS, Verkuilen J, Schwartz MF. Where is the effect of frequency in word production? Insights from aphasic picture naming errors. *Cognitive Neuropsychology*. 2008; 25:463–492. [PubMed: 18704797]

- Lancaster JL, Woldorff MG, Parsons LM, Liotti M, Freitas CS, Rainey L, et al. Automated Talairach atlas labels for functional brain mapping. *Human Brain Mapping*. 2000; 10:120–131. [PubMed: 10912591]
- Léger A, Démonet J-F, Ruff S, Aithamon B, Touyeras B, Puel M, et al. Neural substrates of spoken language rehabilitation in an aphasic patient: An fMRI study. *Neuroimage*. 2002; 17:174–183. [PubMed: 12482075]
- Levelt WJM. Spoken word production: A theory of lexical access. *Proceedings of the National Academy of Sciences, U.S.A.* 2001; 98:13464–13471.
- Martin PI, Naeser MA, Doron KW, Bogdan A, Baker EH, Kurland J, et al. Overt naming in aphasia studied with a functional MRI hemodynamic delay design. *Neuroimage*. 2005; 28:194–204. [PubMed: 16009568]
- Meinzer M, Flaisch T, Breitenstein C, Wienbruch C, Elbert T, Rockstroh B. Functional re-recruitment of dysfunctional brain areas predicts language recovery in chronic aphasia. *Neuroimage*. 2008; 39:2038–2046. [PubMed: 18096407]
- Meinzer M, Flaisch T, Obleser J, Assadollahi R, Djundja D, Barthel G, et al. Brain regions essential for improved lexical access in an aged aphasic patient: A case report. *BMC Neurology*. 2006; 17:6–28.
- Naeser MA, Martin PI, Baker EH, Hodge SM, Sczerzenie SE, Nicholas M, et al. Overt propositional speech in chronic nonfluent aphasia studied with the dynamic susceptibility contrast fMRI method. *Neuroimage*. 2004; 22:29–41. [PubMed: 15109995]
- Naeser MA, Martin PI, Nicholas M, Baker EH, Seekins H, Kobayashi M, et al. Improved picture naming in chronic aphasia after TMS to part of right Broca's area: An open-protocol study. *Brain and Language*. 2005; 93:95–105. [PubMed: 15766771]
- Ohyama M, Senda M, Kitamura S, Ishii K, Mishina M, Terashi A. Role of the nondominant hemisphere and undamaged area during word repetition in poststroke aphasics: A PET activation study. *Stroke*. 1996; 27:897–903. [PubMed: 8623110]
- Perani D, Cappa SF, Tettamanti M, Rosa M, Scifo P, Miozzo A, et al. A fMRI study of word retrieval in aphasia. *Brain and Language*. 2003; 85:357–368. [PubMed: 12744947]
- Rao SM, Binder JR, Bandettini PA, Hammeke TA, Yetkin FZ, Jesmanowicz A, et al. Functional magnetic resonance imaging of complex human movements. *Neurology*. 1993; 43:2311–2318. [PubMed: 8232948]
- Rosen HJ, Petersen SE, Linenweber MR, Snyder AZ, White DA, Chapman L, et al. Neural correlates of recovery from aphasia after damage to left inferior frontal cortex. *Neurology*. 2000; 55:1883–1894. [PubMed: 11134389]
- Saur D, Lange R, Baumgaertner A, Schraknepper V, Willmes K, Rijntjes M, et al. Dynamics of language reorganization after stroke. *Brain*. 2006; 129:1371–1384. [PubMed: 16638796]
- Schnur TT, Schwartz MF, Brecher A, Hodgson C. Semantic interference during blocked-cyclic naming. Evidence from aphasia. *Journal of Memory and Language*. 2006; 54:199–227.
- Schwartz MF, Dell GS, Martin N, Gahl S, Sobel P. A case-series test of the interactive two-step model of lexical access: Evidence from picture naming. *Journal of Memory and Language*. 2006; 54:228–264.
- Solomon J, Raymond V, Braun A, Butman JA, Grafman J. User-friendly software for the analysis of brain lesions (ABLE). *Computer Methods and Programs in Biomedicine*. 2007; 86:245–254. [PubMed: 17408802]
- Szekely A, Jacobsen T, D'Amico S, Devescovi A, Andonova E, Herron D, et al. A new on-line resource for psycholinguistic studies. *Journal of Memory and Language*. 2004; 51:247–250. [PubMed: 23002322]
- Talairach, J.; Tournoux, P. *Co-planar stereotaxic atlas of the human brain*. New York: Thieme; 1988.
- Thulborn KR, Carpenter PA, Just MA. Plasticity of language-related brain function during recovery from stroke. *Stroke*. 1999; 30:749–754. [PubMed: 10187873]
- Tzourio-Mazoyer N, Landeau B, Papathanassiou D, Crivello F, Etard O, Delcroix N, et al. Automated anatomical labeling of activations in SPM using a macroscopic anatomical parcellation of the MNI MRI single-subject brain. *Neuroimage*. 2002; 15:273–289. [PubMed: 11771995]

- Van Lancker Sidtis D, Postman WA. Formulaic expressions in spontaneous speech of left-and right-hemisphere damaged subjects. *Aphasiology*. 2006; 20:411–426.
- Vitali P, Abutalebi J, Tettamanti M, Danna M, Ansaldo A-I, Perani D, et al. Training-induced brain remapping in chronic aphasia: A pilot study. *Neurorehabilitation and Neural Repair*. 2007; 21:152–160. [PubMed: 17312090]
- Warburton E, Price CJ, Swinburn K, Wise RJ. Mechanisms of recovery from aphasia: Evidence from positron emission tomography studies. *Journal of Neurology, Neurosurgery and Psychiatry*. 1999; 66:155–161.
- Winhuisen L, Thiel A, Schumacher B, Kessler J, Rudolf J, Haupt WF, et al. Role of the contralateral inferior frontal gyrus in recovery of language function in poststroke aphasia: A combined repetitive transcranial magnetic stimulation and positron emission tomography study. *Stroke*. 2005; 36:1759–1763. [PubMed: 16020770]

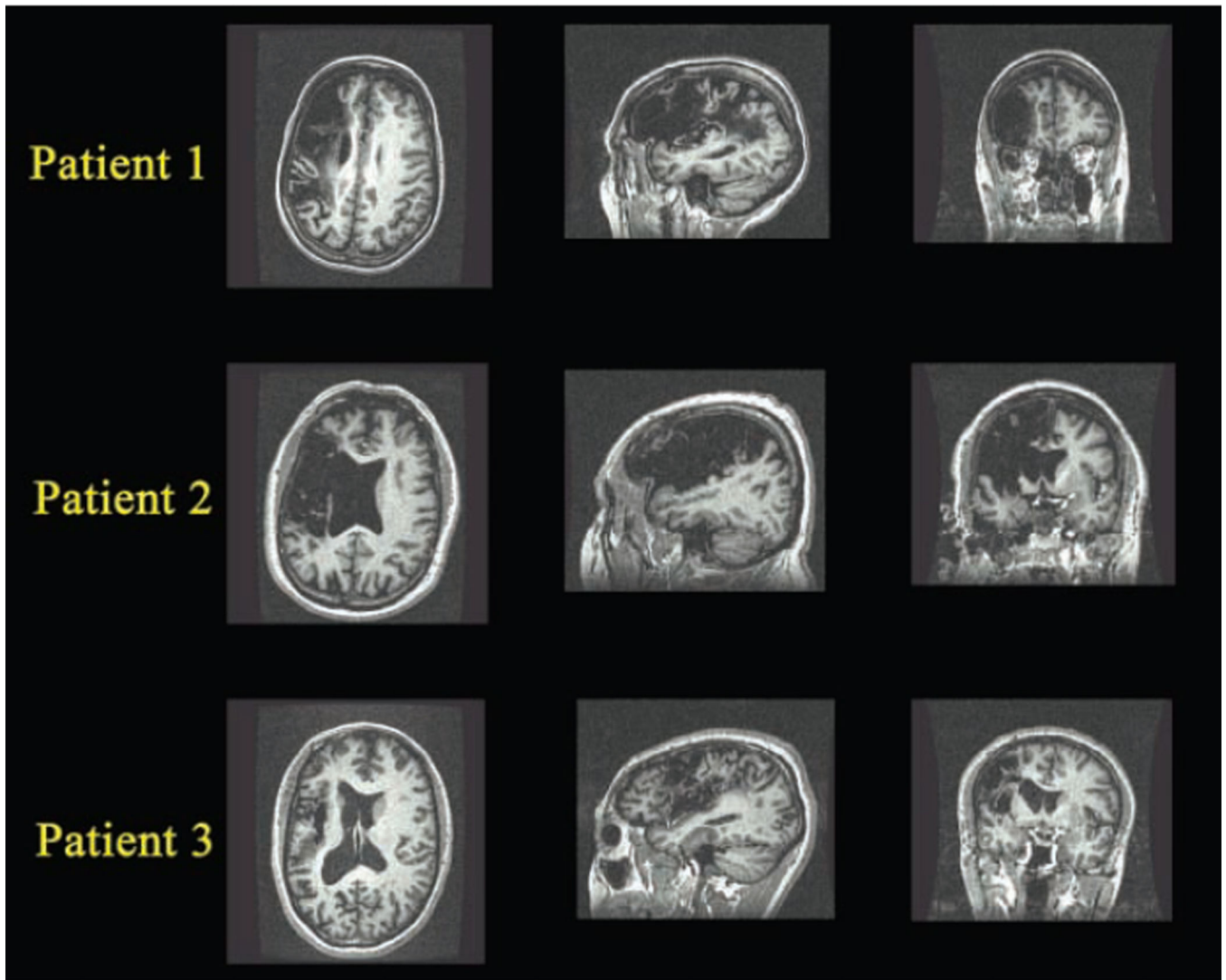


Figure 1.

Axial, sagittal, and coronal views of MP-RAGE scans from each of the three participants with aphasia secondary to stroke, displayed in native space (without stereotaxic normalization). For all three patients, lesions were entirely left-sided, affecting primarily frontal, insular, and temporo-parietal cortices. Images are oriented according to neurologic convention, which is used throughout, with the left side of the image corresponding to the patient's left side.

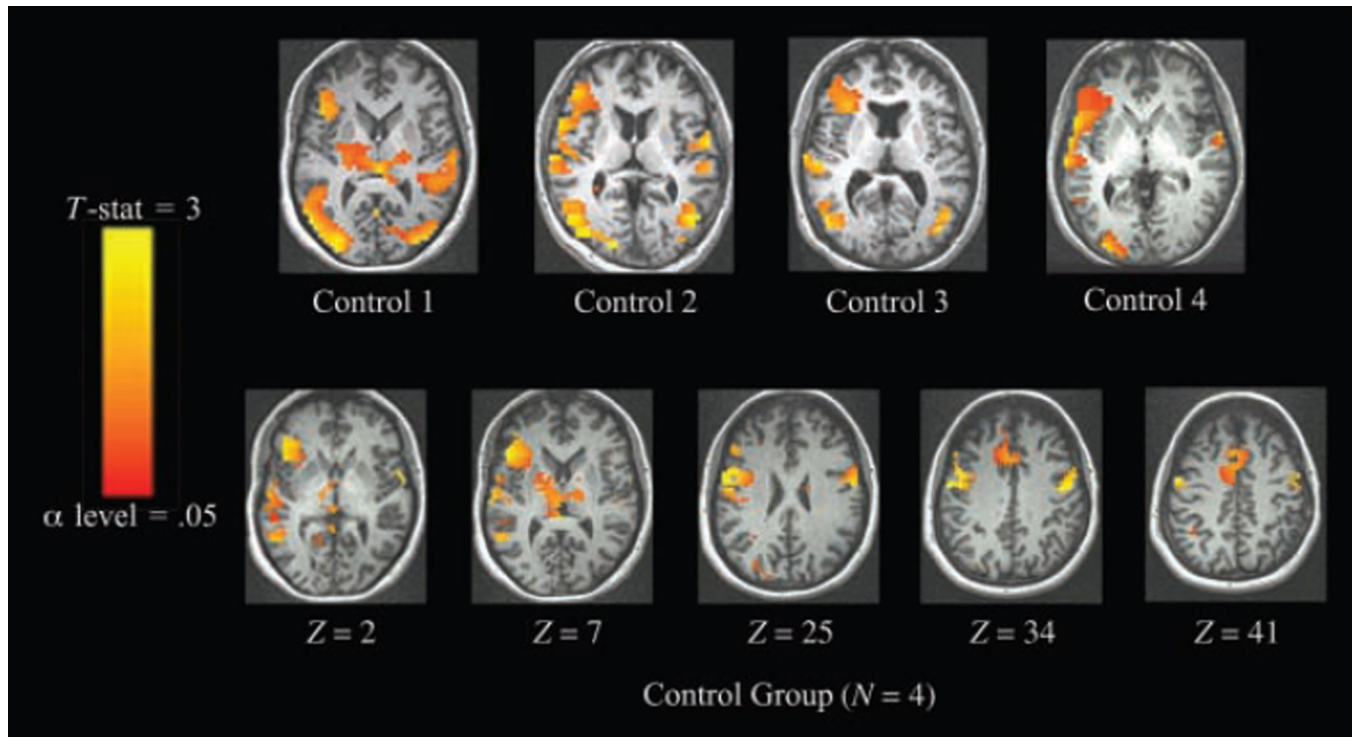


Figure 2. Activation for picture naming > fixation in age-matched control subjects (threshold $\alpha = .05$, corrected cluster level). Individual and grouped data sets were registered to standard Talairach–Tournoux space, with left hemisphere shown on left side of figure. Above: subject-specific analyses. Below: cohort analysis.

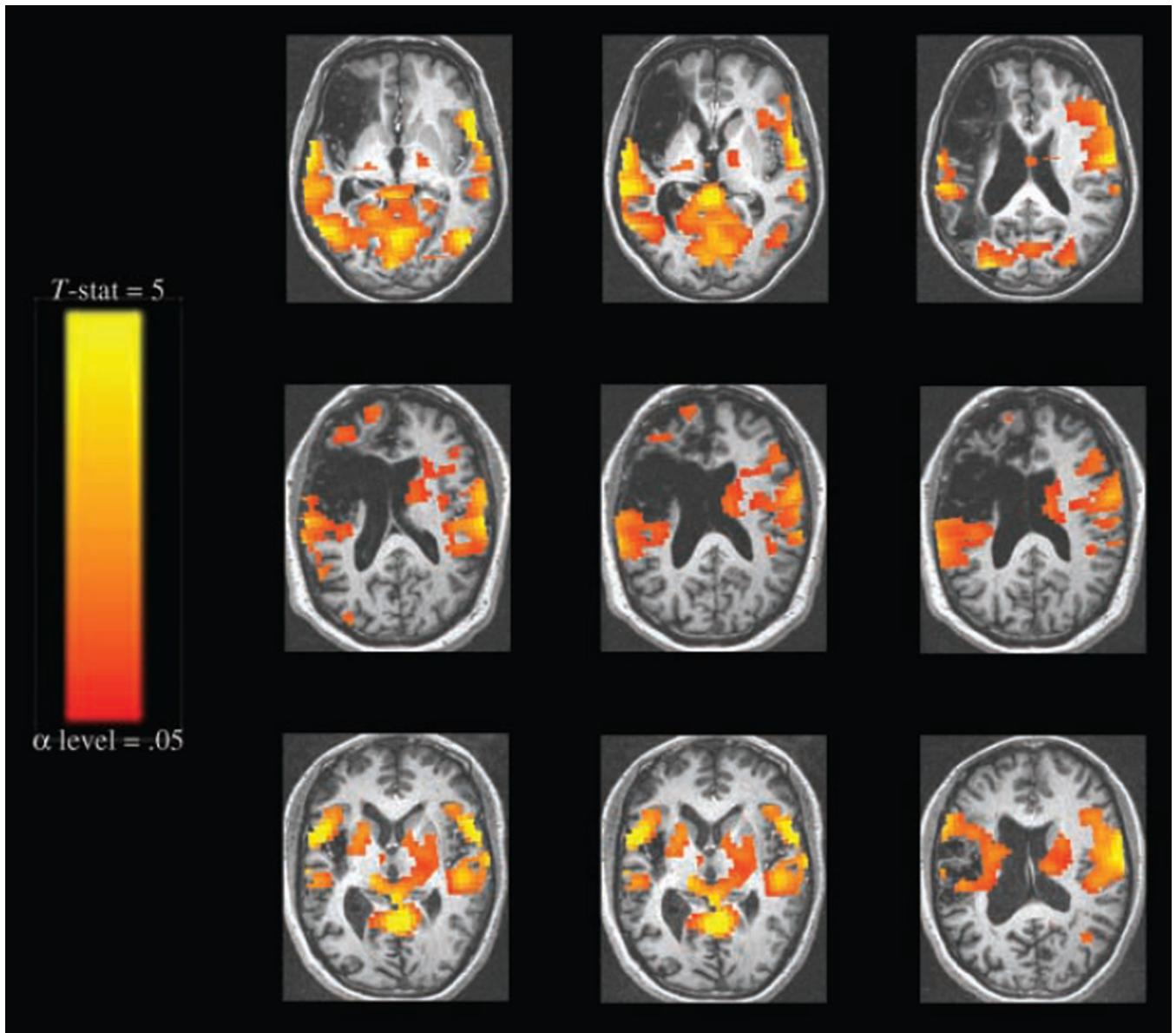


Figure 3. Activation for picture naming > fixation by patients, combining correct and incorrect responses (threshold $\alpha = .05$, corrected cluster level). Images are displayed in standard Talairach–Tournoux space and oriented according to neurologic convention (left hemisphere represented on left side of image). Top row: patient 1; middle row: patient 2; bottom row: patient 3.

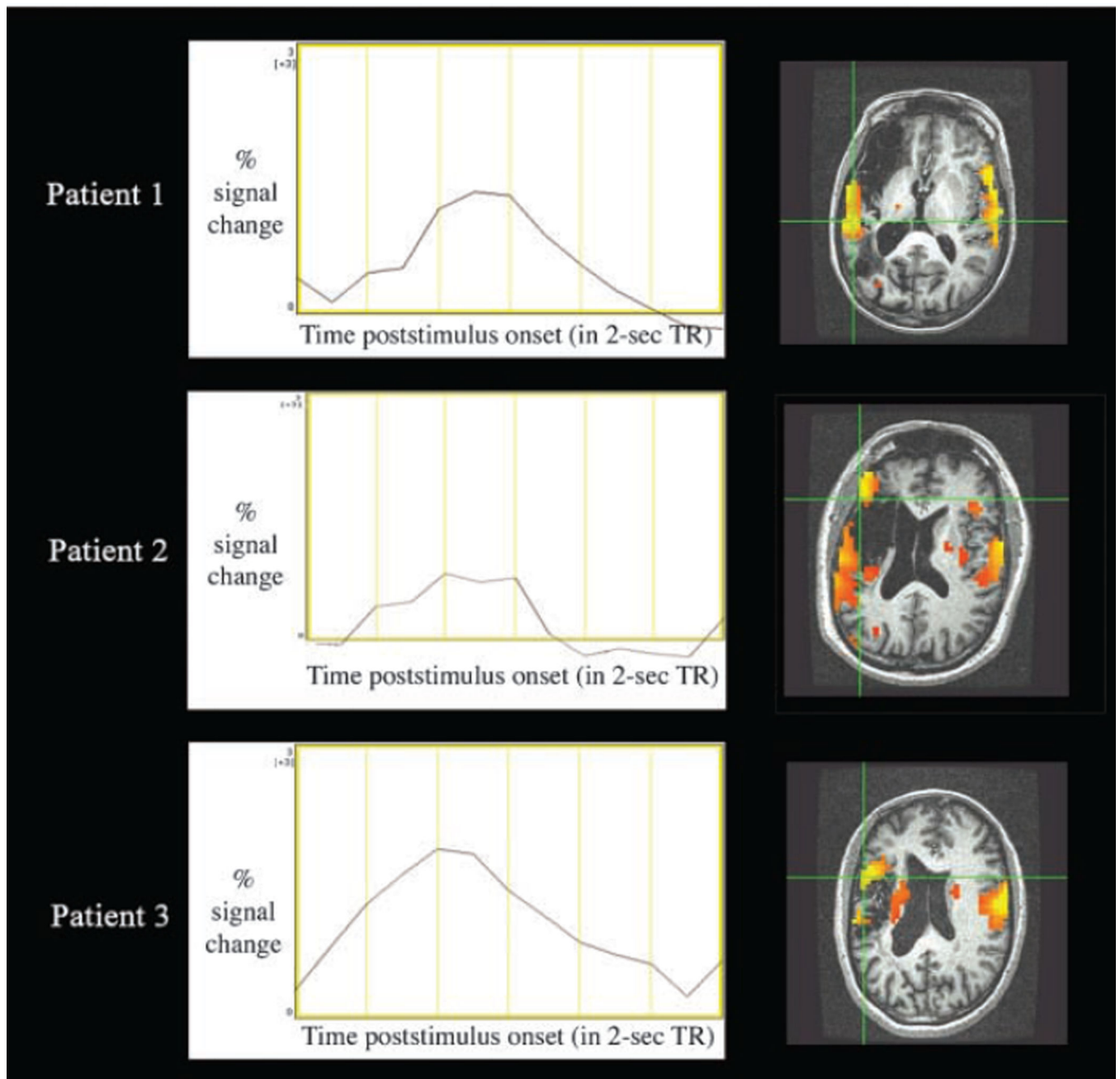


Figure 4. Hemodynamic response in perilesional areas in patients with aphasia. Curves represent estimated impulse response function at corresponding crosshairs. In IRF graphs, baseline is set to global mean of zero on y-axis, which bisects x-axis at the onset of picture stimuli (i.e., time poststimulus onset = 0). Yellow grid lines represent TRs of 2 sec. Images are displayed in native space (without stereotaxic normalization) to generate IRFs from singular perilesional voxels without compromising integrity of lesion extent and shape.

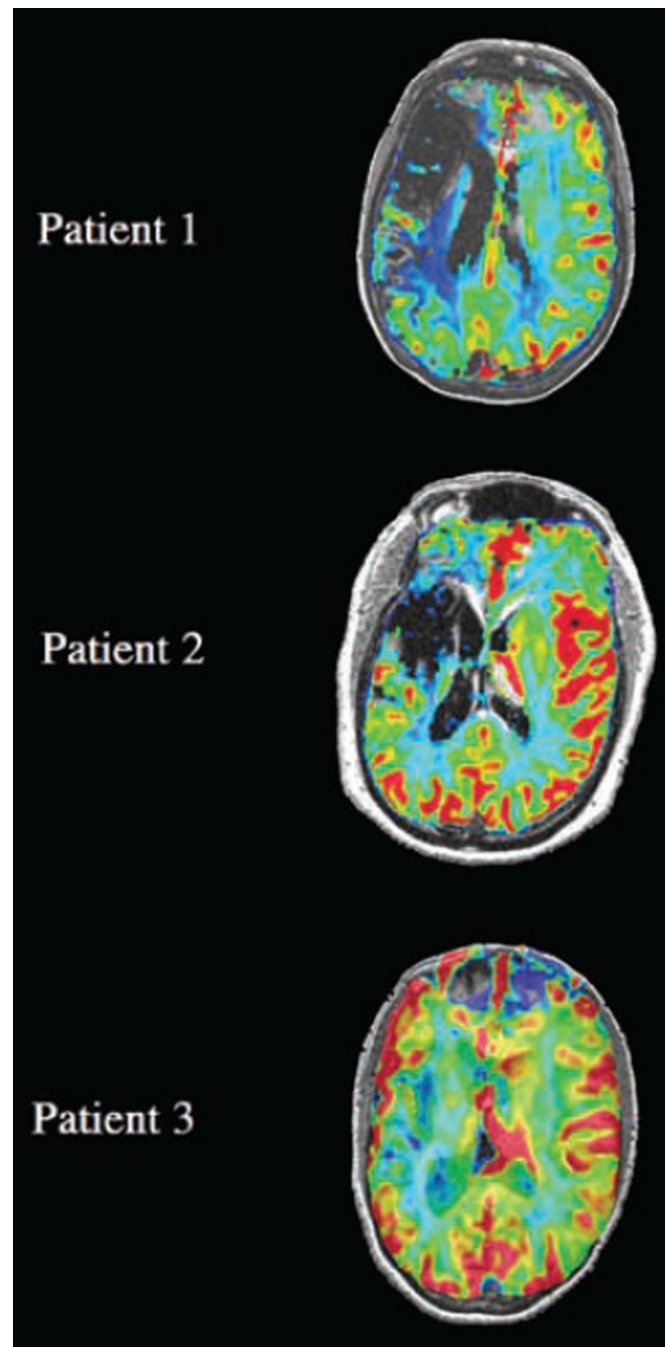


Figure 5. Relative CBF maps demonstrating perilesional perfusion in aphasic patients are superimposed on the T1-weighted anatomical images (gray scale) at levels corresponding to those shown in Figure 3 (see Methods). Images are shown in native space (without stereotaxic normalization), preserving integrity of lesion extent and shape. Perfusion to perilesional cortex is evident in all three cases. Relative CBF was greater than that of white matter, approaching the flow levels of gray matter in the contralateral hemisphere at the sites of activation identified in the BOLD fMRI contrasts (Figures 3 and 4) in each patient. On

this normalized color scale, normal white matter perfusion is seen in the blue to green range and normal gray matter perfusion is seen in the yellow-red range. Note that there is absent blood flow corresponding to the site of infarct (low signal intensity comparable to CSF on the T1 image) in each case.

Author Manuscript

Author Manuscript

Author Manuscript

Author Manuscript

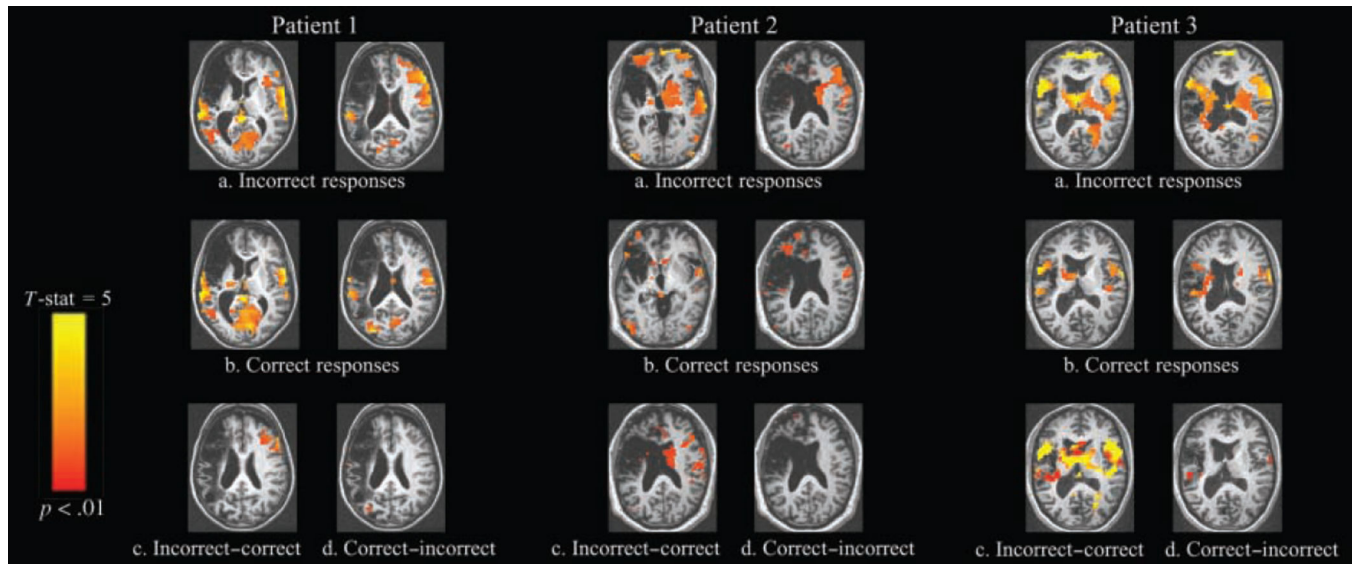


Figure 6. Comparison of activation patterns for accurate versus inaccurate responses in Patient 1, Patient 2, and Patient 3 showing activation for (a) incorrect responses > fixation; (b) correct responses > fixation; (c) incorrect - fixation > correct - fixation; and (d) correct - fixation > incorrect - fixation contrasts (threshold $p < .01$, corrected cluster level). Images are displayed in standard Talairach–Tournoux space. In the case of Patient 3, more motion-related noise was observed. However, this was not seen in the areas of contralesional activation but rather at the edge of the superior frontal cortex.

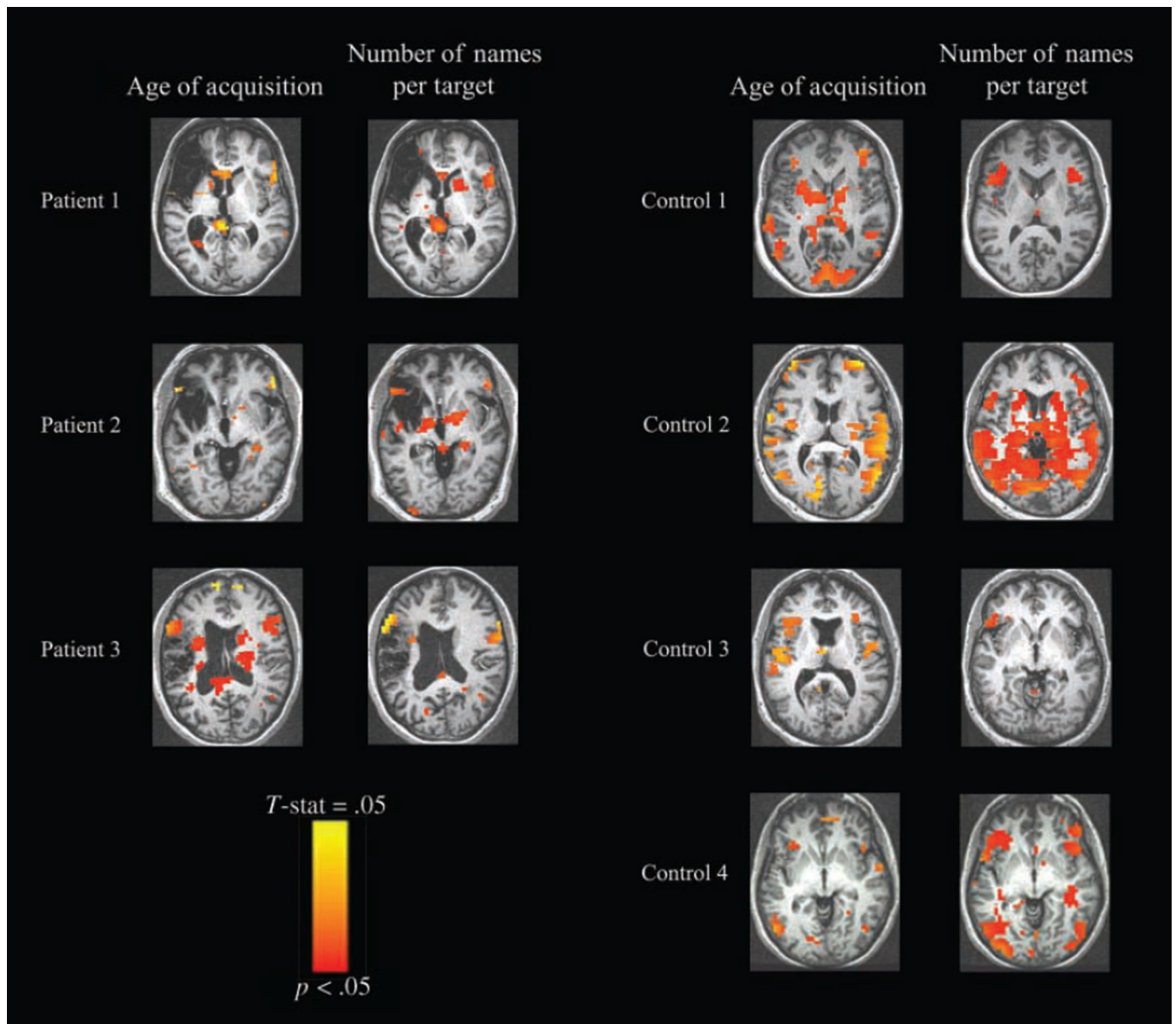


Figure 7. Results of amplitude modulated regression showing active voxels for picture naming whose activation level was also modulated by AoA and number of names per target. Suprathreshold voxels are those showing increasing BOLD signal with increasing AoA and number of names per target values for the picture stimuli. Left panel: results for each of the patients. Right panel: results for each of the age-matched control subjects (threshold $p < .05$). Images are displayed in standard Talairach–Tournoux space.

Background Information, Aphasia Type and Behavioral Scores for the Participants Selected for Analysis

Table 1

	Sex	Age (years)	Years after onset	WAB Naming (%)	WAB Repetition (%)	PALPA Picture Matching (%)	PAL Semantic Probe (%)
Patient 1	F	68	9	70	65	98	94
Patient 2	M	63	4	77	88	100	94
Patient 3	F	48	3	90	88	98	98

Scores for each participant are from subtests of single word production and comprehension (WAB = Western Aphasia Battery; PALPA = Psycholinguistic Assessment of Language Processing in Aphasia; PAL = Psycholinguistic Assessment of Language).

Table 2

Analysis of Brain Lesion Results for Three Patients with Aphasia Showing Total Volume Loss and Fraction Loss by Gyrus in Left Hemisphere for Patients

	Patient 1	Patient 2	Patient 3
Left hemisphere volume loss (μ l)	98	136	76
Percentage loss of total brain volume	6.99	7.80	5.40
AAL region of interest fraction loss			
Left superior frontal gyrus	0.61	29.87	0.00
Left middle frontal gyrus	31.73	27.49	17.97
Left middle frontal orbital gyrus	39.41	1.35	0.00
Left inferior frontal opercular gyrus	88.54	86.13	95.18
Left inferior frontal triangular gyrus	84.90	68.49	24.28
Left inferior frontal orbital gyrus	70.83	28.11	0.00
Left rolandic opercular gyrus	88.69	90.00	91.72
Left insula gyrus	80.79	90.15	34.93
Left precentral gyrus	37.18	77.45	43.96
Left postcentral gyrus	25.33	67.55	35.87
Left inferior parietal gyrus	30.65	31.43	38.78
Left supramarginal gyrus	40.37	27.23	91.16
Left angular gyrus	30.09	0.00	24.47
Left putamen	4.76	67.69	0.10
Left pallidum	0.00	24.23	0.00
Left Heschl's gyrus	36.89	44.00	41.78
Left superior temporal gyrus	14.42	7.14	64.90

Table 3

Naming Performance during Scanning by the Participants with Aphasia

	% Correct	% Semantic Errors	% Phonemic Errors	% Omissions
Patient 1	53% (76 trials)	22% (31 trials)	5% (8 trials)	20% (29 trials)
Patient 2	76% (109 trials)	15% (21 trials)	1% (2 trials)	8% (12 trials)
Patient 3	73% (104 trials)	10% (15 trials)	2% (3 trials)	15% (22 trials)

Author Manuscript

Author Manuscript

Author Manuscript

Author Manuscript

Table 4

Talairach Atlas Labels (Lancaster et al., 2000) and Coordinates for Points of Maximal Activation for Picture Naming > Fixation in Cohort Analysis of Healthy Age-matched Control Subjects ($n = 4$) in Areas Matching Contralesional and Perilesional Regions in Patients

Label and Brodmann's Area	Focus Point (LPI Orientation)	t Statistics
Left superior frontal gyrus (BA 6)	-1 mm [L], 16 mm [A], 62 mm [S]	2.64
Left medial frontal gyrus (BA 6)	-1 mm [L], -0 mm [P], 52 mm [S]	2.25
Left middle frontal gyrus (BA 9)	-45 mm [L], 10 mm [A], 31 mm [S]	2.59
Left middle frontal gyrus (BA 46)	-44 mm [L], 30 mm [A], 15 mm [S]	2.46
Left inferior frontal gyrus (BA 47)	-40 mm [L], 33 mm [A], 1 mm [S]	2.31
Left inferior frontal gyrus (BA 45)	-48 mm [L], 23 mm [A], 6 mm [S]	2.94
Left inferior frontal gyrus (BA 44)	-56 mm [L], 10 mm [A], 18 mm [S]	2.33
Left precentral gyrus (BA 6)	-52 mm [L], -3 mm [P], 39 mm [S]	3.36
Left precentral gyrus (BA 6)	-57 mm [L], 2 mm [A], 29 mm [S]	4.66
Right superior frontal gyrus (BA 6)	1 mm [R], 5 mm [A], 68 mm [S]	3.59
Right middle frontal gyrus (BA 6)	56 mm [R], 4 mm [A], 41 mm [S]	3.34
Right precentral gyrus (BA 6)	52 mm [R], -8 mm [P], 27 mm [S]	3.67

LPI = left-to-right, posterior-to-anterior, inferior-to-superior.

Table 5

Talairach Atlas Labels and Coordinates for Points of Maximal Activation in Perilesional and Contralateral Regions for Picture Naming (All Responses, Both Accurate and Inaccurate) > Fixation in Each of the Three Participants with Aphasia: Patient 1, Patient 2, and Patient 3

Label and Brodmann's Area	Focus Point (LPI)	t Statistics	Patient
Left superior frontal gyrus (BA 10)	-12 mm [L], 67 mm [A], -3 mm [I]	4.34	Patient 2
Left superior frontal gyrus (BA 6)	-9 mm [L], 14 mm [A], 63 mm [S]	4.68	Patient 1
Left superior frontal gyrus (BA 6)	-9 mm [L], 2 mm [A], 65 mm [S]	5.52	Patient 3
Left medial frontal gyrus (BA 6)	-6 mm [L], 17 mm [A], 42 mm [S]	4.11	Patient 1
Left middle frontal gyrus (BA 9)	-29 mm [L], 43 mm [A], 34 mm [S]	7.47	Patient 1
Left middle frontal gyrus (BA 9)	-52 mm [L], 19 mm [A], 32 mm [S]	4.76	Patient 3
Left middle frontal gyrus (BA 47)	-47 mm [L], 48 mm [A], -9 mm [I]	4.8	Patient 2
Left inferior frontal gyrus (BA 47)	-54 mm [L], 34 mm [A], -10 mm [I]	5.91	Patient 2
Left inferior frontal gyrus (BA 47)	-46 mm [L], 30 mm [A], -8 mm [I]	6.87	Patient 3
Left inferior frontal gyrus (BA 44)	-52 mm [L], 16 mm [A], 11 mm [S]	4.84	Patient 3
Left precentral gyrus (BA 6)	-62 mm [L], -9 mm [P], 30 mm [S]	6.89	Patient 1
Left precentral gyrus (BA 6)	-60 mm [L], -0 mm [P], 12 mm [S]	7.01	Patient 3
Left precentral gyrus (BA 4)	-38 mm [L], -25 mm [P], 62 mm [S]	9.47	Patient 1
Right superior frontal gyrus (BA 6)	13 mm [R], 4 mm [A], 66 mm [S]	3.8	Patient 1
Right superior frontal gyrus (BA 6)	18 mm [R], 12 mm [A], 66 mm [S]	4.14	Patient 2
Right medial frontal gyrus (BA 10)	20 mm [R], 63 mm [A], -5 mm [I]	5.23	Patient 2
Right medial frontal gyrus (BA 6)	1 mm [R], -6 mm [P], 49 mm [S]	6.16	Patient 1
Right middle frontal gyrus (BA 11)	43 mm [R], 33 mm [A], -8 mm [I]	4.53	Patient 3
Right middle frontal gyrus (BA 6)	36 mm [R], 3 mm [A], 58 mm [S]	4.72	Patient 2
Right IFG (BA 9)	50 mm [R], -1 mm [P], 22 mm [S]	4.14	Patient 2
Right IFG (BA 47)	45 mm [R], 23 mm [A], -14 mm [I]	6.5	Patient 1
Right IFG (BA 47)	51 mm [R], 18 mm [A], -5 mm [I]	8.11	Patient 3
Right IFG (BA 45)	53 mm [R], 15 mm [A], 0 mm [S]	9.49	Patient 1
Right IFG (BA 45)	47 mm [R], 20 mm [A], 12 mm [S]	4.74	Patient 3
Right IFG (BA 44)	62 mm [R], 9 mm [A], 18 mm [S]	4.85	Patient 3
Right precentral/IFG (BA 44)	62 mm [R], 11 mm [A], 11 mm [S]	4.63	Patient 2
Right precentral gyrus (BA 6)	49 mm [R], 3 mm [A], 33 mm [S]	5.39	Patient 2
Right precentral gyrus (BA 6)	58 mm [R], -5 mm [P], 34 mm [S]	6.92	Patient 1
Right precentral gyrus (BA 6)	62 mm [R], -2 mm [P], 25 mm [S]	9.28	Patient 3
Right precentral gyrus (BA 4)	42 mm [R], -9 mm [P], 56 mm [S]	6.83	Patient 2
Right precentral gyrus (BA 4)	48 mm [R], -11 mm [P], 49 mm [S]	6.02	Patient 3

Table 6

Talairach Atlas Labels and Coordinates for Points of Maximal Activation in Perilesional and Contralateral Regions for Correct Picture Naming > Fixation in Each of the Three Participants with Aphasia

Label and Nearest Brodmann's Area	Focus Point (LPI)	t Statistics	Patient
Left superior frontal gyrus (BA 6)	-9 mm [L], 14 mm [A], 63 mm [S]	4.14	Patient 1
Left superior frontal gyrus (BA 6)	-7 mm [L], -15 mm [P], 67 mm [S]	3.23	Patient 3
Left medial frontal gyrus (BA 6)	-1 mm [L], -12 mm [P], 67 mm [S]	2.05	Patient 2
Left precentral gyrus (BA 4)	-63 mm [L], -5 mm [P], 19 mm [S]	5.3	Patient 1
Left precentral gyrus (BA 4)	-43 mm [L], -18 mm [P], 38 mm [S]	3.62	Patient 3
Right superior frontal gyrus (BA 6)	29 mm [R], -6 mm [P], 67 mm [S]	3.77	Patient 2
Right medial frontal gyrus (BA 6)	1 mm [R], -6 mm [P], 49 mm [S]	4.37	Patient 1
Right precentral gyrus (BA 6)	58 mm [R], -5 mm [P], 34 mm [S]	4.67	Patient 1
Right precentral gyrus (BA 6)	56 mm [R], -4 mm [P], 43 mm [S]	5.54	Patient 2
Right precentral gyrus (BA 6)	62 mm [R], -2 mm [P], 25 mm [S]	7.06	Patient 3
Right precentral gyrus (BA 4)	45 mm [R], -11 mm [P], 49 mm [S]	3.97	Patient 3
Right precentral gyrus (BA 4)	61 mm [R], -5 mm [P], 20 mm [S]	3.77	Patient 1

Table 7

Talairach Atlas Labels and Coordinates for Points of Maximal Activation in Perilesional and Contralateral Regions for Incorrect Picture Naming > Fixation in Each of the Three Participants with Aphasia

Label and Nearest Brodmann's Area	Focus Point (LPI)	t Statistics	Patient
Left superior frontal gyrus (BA 10)	-15 mm [L], 65 mm [A], -7 mm [I]	5.56	Patient 2
Left superior frontal gyrus (BA 6)	-4 mm [L], 10 mm [A], 64 mm [S]	4.52	Patient 1
Left superior frontal gyrus (BA 6)	-5 mm [L], 6 mm [A], 65 mm [S]	5.73	Patient 3
Left medial frontal gyrus (BA 6)	-7 mm [L], -2 mm [P], 52 mm [S]	4.51	Patient 1
Left middle frontal gyrus (BA 9)	-48 mm [L], 19 mm [A], 32 mm [S]	5.57	Patient 3
Left IFG (BA 47)	-46 mm [L], 17 mm [A], 0 mm [S]	5.3	Patient 3
Left IFG (BA 45)	-61 mm [L], 23 mm [A], 10 mm [S]	7.24	Patient 3
Left inferior frontal/precentral gyrus (BA 44/6)	-64 mm [L], 11 mm [A], 9 mm [S]	11.99	Patient 3
Right superior frontal gyrus (BA 6)	29 mm [R], -6 mm [P], 67 mm [S]	6.12	Patient 2
Right medial frontal gyrus (BA 6)	1 mm [R], -6 mm [P], 49 mm [S]	5.39	Patient 1
Right middle frontal gyrus (BA 6)	47 mm [R], 3 mm [A], 53 mm [S]	5.04	Patient 2
Right middle frontal gyrus (BA 46)	51 mm [R], 24 mm [A], 25 mm [S]	4.6	Patient 1
Right middle frontal gyrus (BA 9)	37 mm [R], 49 mm [A], 28 mm [S]	5.04	Patient 2
Right middle/IFG (BA 9)	54 mm [R], 10 mm [A], 27 mm [S]	3.66	Patient 3
Right middle/IFG (BA 10)	44 mm [R], 56 mm [A], 0 mm [S]	3.5	Patient 2
Right IFG (BA 44)	55 mm [R], 16 mm [A], 19 mm [S]	3.85	Patient 1
Right IFG (BA 44)	52 mm [R], 4 mm [P], 22 mm [S]	2.35	Patient 2
Right IFG (BA 44)	61 mm [R], 9 mm [A], 17 mm [S]	5.22	Patient 3
Right IFG (BA 45)	48 mm [R], 24 mm [A], 11 mm [S]	5.19	Patient 3
Right precentral gyrus (BA 44)	57 mm [R], 6 mm [A], 13 mm [S]	3.63	Patient 1
Right precentral gyrus (BA 6)	58 mm [R], -5 mm [P], 34 mm [S]	5.21	Patient 1
Right precentral gyrus (BA 4)	45 mm [R], -9 mm [P], 56 mm [S]	6.53	Patient 2
Right precentral gyrus (BA 4)	50 mm [R], -11 mm [P], 44 mm [S]	5.97	Patient 3
Right insula (BA 13)	39 mm [R], 16 mm [A], 12 mm [S]	3.95	Patient 3

Table 8

Talairach Atlas Labels and Coordinates for Points of Maximal Activation in Perilesional and Contralateral Regions Modulated by AoA for Each of the Three Participants with Aphasia

Label and Nearest Brodmann's Area	Focus Point (LPI)	Coefficient	Patient
Left superior frontal gyrus (BA 10)	-11 mm [L], 62 mm [A], 14 mm [S]	0.25	Patient 1
Left superior frontal gyrus (BA 6)	-18 mm [L], 17 mm [A], 62 mm [S]	0.38	Patient 1
Left medial frontal gyrus (BA 6)	-3 mm [L], -15 mm [P], 65 mm [S]	0.43	Patient 3
Left anterior cingulate (BA 32)	-0 mm [L], 28 mm [A], -9 mm [I]	0.42	Patient 1
Left cingulate gyrus (BA 24)	-6 mm [L], -2 mm [P], 34 mm [S]	0.42	Patient 3
Left middle frontal gyrus (BA 11)	-36 mm [L], 51 mm [A], -9 mm [I]	0.45	Patient 1
Left middle/IFG (BA 47)	-33 mm [L], 35 mm [A], -7 mm [I]	0.69	Patient 3
Left inferior/middle frontal gyrus (BA 10)	-34 mm [L], 42 mm [A], 0 mm [S]	0.25	Patient 1
Left inferior/middle frontal gyrus (BA 10/45)	-44 mm [L], 39 mm [A], 0 mm [S]	0.32	Patient 3
Left inferior frontal gyrus (BA 46)	-55 mm [L], 29 mm [A], 17 mm [S]	0.54	Patient 3
Left inferior frontal gyrus (BA 47)	-46 mm [L], 30 mm [A], -8 mm [I]	1.01	Patient 3
Left inferior frontal gyrus (BA 47)	-54 mm [L], 19 mm [A], -4 mm [I]	0.26	Patient 1
Left inferior frontal gyrus (BA 47)	-54 mm [L], 34 mm [A], -10 mm [I]	0.5	Patient 2
Left inferior frontal gyrus (BA 44)	-52 mm [L], 16 mm [A], 11 mm [S]	0.39	Patient 3
Left inferior frontal gyrus (BA 45)	-61 mm [L], 26 mm [A], 6 mm [S]	0.41	Patient 3
Left precentral gyrus (BA 6)	-38 mm [L], -1 mm [P], 40 mm [S]	0.4	Patient 1
Right superior frontal gyrus (BA 10)	27 mm [R], 61 mm [A], -1 mm [I]	3.14	Patient 3
Right superior frontal gyrus (BA 10)	13 mm [R], 66 mm [A], 7 mm [S]	0.26	Patient 1
Right superior frontal gyrus (BA 6)	14 mm [R], 30 mm [A], 53 mm [S]	0.41	Patient 3
Right superior frontal gyrus (BA 6)	5 mm [R], 3 mm [A], 66 mm [S]	0.63	Patient 1
Right Medial/superior frontal gyrus (BA 6)	3 mm [R], -5 mm [P], 62 mm [S]	0.58	Patient 3
Right middle frontal gyrus (BA 10)	42 mm [R], 55 mm [A], -10 mm [I]	0.38	Patient 1
Right middle/IFG (BA 47)	50 mm [R], 41 mm [A], -7 mm [I]	0.5	Patient 2
Right IFG (BA 47)	54 mm [R], 19 mm [A], 0 mm [S]	0.35	Patient 1
Right IFG (BA 44)	61 mm [R], 17 mm [A], 16 mm [S]	0.31	Patient 3
Right IFG (BA 45)	53 mm [R], 29 mm [A], 4 mm [S]	0.3	Patient 1
Right IFG (BA 45)	49 mm [R], 36 mm [A], 1 mm [S]	0.49	Patient 2
Right insula (BA 13)	48 mm [R], 11 mm [A], 2 mm [S]	0.25	Patient 1

Table 9

Talairach Atlas Labels and Coordinates for Points of Maximal Activation in Perilesional and Contralateral Regions Modulated by Number of Names per Target for Each of the Three Patients with Aphasia

Label and Nearest Brodmann's Area	Focus Point (LPI)	Coefficient	Patient
Left superior frontal gyrus (BA 10)	-19 mm [L], 61 mm [A], 16 mm [S]	0.2	Patient 1
Left anterior cingulate (BA 32)	-0 mm [L], 28 mm [A], -9 mm [I]	0.18	Patient 1
Left middle frontal gyrus (BA 8)	-40 mm [L], 29 mm [A], 38 mm [S]	0.14	Patient 1
Left middle frontal gyrus (BA 9)	-52 mm [L], 19 mm [A], 32 mm [S]	0.13	Patient 3
Left inferior frontal gyrus (BA 47)	-53 mm [L], 31 mm [A], -9 mm [I]	0.25	Patient 2
Left inferior frontal gyrus (BA 47)	-50 mm [L], 15 mm [A], 0 mm [S]	0.13	Patient 3
Left inferior frontal gyrus (BA 44)	-61 mm [L], 15 mm [A], 11 mm [S]	0.21	Patient 3
Left inferior frontal gyrus (BA 45)	-57 mm [L], 27 mm [A], 4 mm [S]	0.15	Patient 3
Left precentral gyrus (BA 6)	-63 mm [L], 4 mm [A], 6 mm [S]	0.18	Patient 3
Left precentral gyrus (BA 6)	-38 mm [L], -1 mm [P], 40 mm [S]	0.18	Patient 1
Right superior frontal gyrus (BA 6)	9 mm [R], 3 mm [A], 66 mm [S]	0.23	Patient 1
Right superior frontal gyrus (BA 10)	19 mm [R], 59 mm [A], 23 mm [S]	0.3	Patient 1
Right superior frontal gyrus (BA 10)	38 mm [R], 61 mm [A], 16 mm [S]	0.23	Patient 2
Right superior frontal gyrus (BA 10)	16 mm [R], 66 mm [A], 13 mm [S]	0.39	Patient 3
Right medial/superior frontal gyrus (BA 10)	17 mm [R], 61 mm [A], 4 mm [S]	0.95	Patient 3
Right middle/superior frontal gyrus (BA 10)	37 mm [R], 54 mm [A], 18 mm [S]	0.26	Patient 2
Right middle frontal gyrus (BA 10)	24 mm [R], 51 mm [A], 18 mm [S]	0.15	Patient 1
Right middle frontal gyrus (BA 6)	30 mm [R], -7 mm [P], 60 mm [S]	0.13	Patient 3
Right middle/IFG (BA 47)	51 mm [R], 37 mm [A], -5 mm [I]	0.2	Patient 2
Right middle/IFG (BA 46)	55 mm [R], 23 mm [A], 26 mm [S]	0.17	Patient 1
Right middle/IFG (BA 46/45)	48 mm [R], 26 mm [A], 26 mm [S]	0.11	Patient 3
Right IFG (BA 45/46)	47 mm [R], 38 mm [A], 0 mm [S]	0.2	Patient 2
Right IFG (BA 47)	52 mm [R], 34 mm [A], -11 mm [I]	0.18	Patient 1
Right IFG (BA 45)	55 mm [R], 15 mm [A], 1 mm [S]	0.18	Patient 1

Table 10

Talairach Atlas Labels and Coordinates for Points of Maximal Activation Modulated by AoA for Each of the Four Age-matched Control Subjects in Areas Matching Contralesional and Perilesional Regions in Patients

Label and Nearest Brodmann's Area	Focus Point (LPI)	Coefficient	Subject
Left superior frontal gyrus (BA 6)	-3 mm [L], 3 mm [A], 67 mm [S]	0.82	Control 2
Left superior frontal gyrus (BA 6)	-17 mm [L], 23 mm [A], 57 mm [S]	0.22	Control 1
Left superior frontal gyrus (BA 6/8)	-1 mm [L], 14 mm [A], 53 mm [S]	0.11	Control 4
Left middle frontal gyrus (BA 10)	-38 mm [L], 62 mm [A], 7 mm [S]	0.59	Control 2
Left middle/IFG (BA 10/46)	-39 mm [L], 38 mm [A], 14 mm [S]	0.1	Control 1
Left inferior/middle frontal gyrus (BA 9)	-44 mm [L], 6 mm [A], 29 mm [S]	0.11	Control 4
Left inferior frontal gyrus (BA 9)	-44 mm [L], 7 mm [A], 28 mm [S]	0.13	Control 1
Left inferior frontal gyrus (BA 47)	-36 mm [L], 33 mm [A], 0 mm [S]	0.16	Control 1
Left inferior frontal gyrus (BA 47)	-45 mm [L], 27 mm [A], -16 mm [I]	0.48	Control 2
Left inferior frontal gyrus (BA 47)	-40 mm [L], 20 mm [A], -4 mm [I]	0.11	Control 4
Left inferior frontal gyrus (BA 45)	-32 mm [L], 29 mm [A], 6 mm [S]	0.19	Control 3
Left Precentral/IFG (44/6)	-64 mm [L], 7 mm [A], 12 mm [S]	0.58	Control 2
Left precentral gyrus (BA 4)	-56 mm [L], -11 mm [P], 35 mm [S]	0.1	Control 4
Left precentral gyrus (BA 43/6)	-57 mm [L], -4 mm [P], 11 mm [S]	0.21	Control 3
Left Insula (BA 13)	-44 mm [L], -2 mm [P], 10 mm [S]	0.34	Control 3
Left anterior cingulate (BA 24/32)	-1 mm [L], 39 mm [A], 3 mm [S]	0.19	Control 4
Right medial frontal gyrus (BA 10)	3 mm [R], 54 mm [A], -3 mm [I]	0.24	Control 4
Right middle frontal gyrus (BA 10)	40 mm [R], 55 mm [A], 5 mm [S]	0.41	Control 1
Right middle frontal gyrus (BA 10)	36 mm [R], 62 mm [A], 7 mm [S]	0.76	Control 2
Right middle frontal gyrus (BA 46)	52 mm [R], 44 mm [A], 23 mm [S]	0.23	Control 1
Right inferior/middle frontal gyrus (BA 46/45)	41 mm [R], 35 mm [A], 2 mm [S]	0.11	Control 1
Right IFG (BA 9)	58 mm [R], 15 mm [A], 32 mm [S]	0.13	Control 4
Right IFG (BA 47)	24 mm [R], 14 mm [A], -11 mm [I]	0.8	Control 3
Right IFG (BA 47/45)	54 mm [R], 21 mm [A], -2 mm [I]	0.45	Control 3
Right Precentral/IFG (BA 44)	56 mm [R], 10 mm [A], 7 mm [S]	0.42	Control 3
Right precentral gyrus (BA 44)	46 mm [R], 2 mm [A], 5 mm [S]	0.37	Control 3
Right precentral gyrus (BA 6)	63 mm [R], 4 mm [A], 6 mm [S]	0.44	Control 2
Right precentral gyrus (BA 6)	54 mm [R], -3 mm [P], 13 mm [S]	0.23	Control 3
Right precentral gyrus (BA 6/4)	33 mm [R], -20 mm [P], 63 mm [S]	0.23	Control 1
Right Insula (BA 13)	45 mm [R], 14 mm [A], 4 mm [S]	0.45	Control 3

Table 11

Talairach Atlas Labels and Coordinates for Points of Maximal Activation Modulated by Number of Names per Target for Each of the Four Age-matched Control Subjects in Areas Matching Contralesional and Perilesional Regions in Patients

Label and Nearest Brodmann's Area	Focus Point (LPI)	Coefficient	Patient
Left superior frontal gyrus (BA 9)	-32 mm [L], 47 mm [A], 27 mm [S]	0.15	Control 4
Left superior frontal gyrus (BA 6)	-20 mm [L], -2 mm [P], 66 mm [S]	0.24	Control 4
Left superior/middle frontal gyrus (BA 10)	-20 mm [L], 60 mm [A], 11 mm [S]	0.16	Control 1
Left medial frontal gyrus (BA 10)	-2 mm [L], 65 mm [A], 12 mm [S]	0.23	Control 1
Left medial frontal gyrus (BA 6)	-1 mm [L], -20 mm [P], 67 mm [S]	0.13	Control 4
Left middle frontal gyrus (BA 6)	-45 mm [L], 6 mm [A], 58 mm [S]	0.26	Control 2
Left middle frontal gyrus (BA 9)	-44 mm [L], 25 mm [A], 35 mm [S]	0.12	Control 4
Left middle/IFG (BA 47)	-49 mm [L], 37 mm [A], -4 mm [I]	0.08	Control 4
Left inferior frontal gyrus (BA 45)	-48 mm [L], 19 mm [A], 4 mm [S]	0.11	Control 1
Left inferior frontal gyrus (BA 45/47)	-48 mm [L], 29 mm [A], 3 mm [S]	0.09	Control 3
Left inferior frontal gyrus (BA 47)	-54 mm [L], 22 mm [A], -5 mm [I]	0.17	Control 3
Left inferior frontal gyrus (BA 47/45)	-53 mm [L], 22 mm [A], 1 mm [S]	0.1	Control 4
Left precentral/middle frontal gyrus (BA 6)	-34 mm [L], -7 mm [P], 61 mm [S]	0.19	Control 4
Right superior frontal gyrus (BA 6)	20 mm [R], -4 mm [P], 66 mm [S]	0.07	Control 1
Right superior frontal gyrus (BA 6)	27 mm [R], -2 mm [P], 66 mm [S]	0.37	Control 4
Right medial frontal gyrus (BA 6)	3 mm [R], -3 mm [P], 59 mm [S]	0.06	Control 1
Right middle/IFG (BA 47/10)	50 mm [R], 44 mm [A], -6 mm [I]	0.13	Control 4
Right middle/IFG (BA 11/47)	48 mm [R], 41 mm [A], -17 mm [I]	0.21	Control 2
Right IFG (BA 47)	50 mm [R], 24 mm [A], -5 mm [I]	0.13	Control 4
Right IFG (BA 44/45)	44 mm [R], 19 mm [A], 6 mm [S]	0.05	Control 1
Right precentral gyrus (BA 6)	43 mm [R], -7 mm [P], 61 mm [S]	0.11	Control 4